

Contents lists available at ScienceDirect

# Structures

journal homepage: www.elsevier.com/locate/structures





# Behavior of hot-cast anchor sockets for prestressed cable structures under fire

YANG Hang<sup>a</sup>, ZHU Mei-chun<sup>a,\*</sup>, MENG Fan-qin<sup>b</sup>

- <sup>a</sup> Architecture Engineering School, Shanghai Normal University, Shanghai 201418, China
- <sup>b</sup> Faculty of Engineering, University of Auckland, Auckland 1023, New Zealand

#### ARTICLE INFO

Keywords:
Hot-cast anchor
Fire test
Critical temperature
Temperature field distribution
Finite element simulation

#### ABSTRACT

Zn-Cu alloy filled hot cast anchor sockets are the main link in prestressed cable systems, which could be a significant safety issue without appropriate structural fire design. Thus, two full-scale specimens were heated and loaded until failure to assess the fire performance of the sockets herein. Experimental results show that the temperature of Zn-Cu alloy filler decreases gradually from the bottom to the top along the central axis of sockets, thus Zn-Cu alloy at the bottom of the sockets will melt first. The whole slip process of hot-cast anchor under fire comprises three stages as non-slip, stable growth and sharp acceleration. In the test, the critical temperature of the hot-cast anchors is 374  $^{\circ}$ C – 387  $^{\circ}$ C, and conservatively taken as 350  $^{\circ}$ C. Then, a numerical model was developed and validated through general finite element software ABAQUS, through which the effects of the heating curves, specimen dimensions and steel wire bundle types on fire resistance are further explored. The simulation results reveal that the heating curves and specimen dimensions have significant influence on fire resistance of the specimens, whereas the effect of steel wire bundle types can be neglected. Compared with other heating curves, changing the dimensions has the most obvious effect on the fire resistance of the specimen under the action of HC heating curve.

## 1. Introduction

Large-span and open space structures have been widely developed in the past several decades with the rapid development of the economy. Cable structures with high-strength steel cables as the primary load-bearing elements have become increasingly prevalent in stadiums, exposition centers, and other public buildings. However, cable structures are vulnerable to fire like other steel constructional components. The cable structure consists of two parts, the cable and the anchor, the cable bears the tension and the anchor transmits the tension. Therefore, a reliable anchor connection between the two is a prerequisite to ensuring structural stability in the ultimate limited state [1–3]. The filling materials such as low melting point alloy and resin in the anchors are the weakest link of the cable structures against fire [4–5]. Accurately determining the temperature distribution of the fillers within the anchors and the bonding between the fillers and the cables at high temperatures is crucial for minimizing the fire loss of large-span cable systems.

At present, the research on fire resistance of cable structures is mainly focused on the heating curves and the temperature field distribution of cable sections [6–10], the high-temperature performance of cable materials [11–13], and the overall mechanical performance of cable structures encounters fire [14]. In the scope of the author's literature search, it is only found that the high-temperature performance of cable anchorage system has been tested in literature [4–5,15–16], and the anchorage performance of prestressed steel bar clamp anchor under fire was investigated though the experiments [17].

Klein (2008) [4] researched the fire resistance of wire rope anchoring components widely used in American bridge structures, and tested the specimens of anchorage systems at high temperatures, the filling materials include metal zinc and resin. The results show that fire resistance of the anchorage systems filled with resin is the worst, the resin starts to burn at about 210 °C and the anchorage system fails at 272 °C, while the metal zinc loses the bonding property at 296 °C and the anchorage system fails. Ridge (2012) et al. [5] researched the anchorage systems of British cable structures, and the filling materials include Zn-Al-Cu alloy and Wirelock resin. The results show that when the stress level is 0.4, the critical temperature of the hot-cast anchor is between 210 °C and 223 °C, the critical temperature of the Wirelock anchor is 160 °C, and the anchorage systems will be destroyed within 60 h. It should be

E-mail address: zhumeichun@shnu.edu.cn (Z. Mei-chun).

<sup>\*</sup> Corresponding author.

**Table 1**Parameters and Test Result of Specimens.

Case ID	Filling Material	Specification of Cable	Nominal Diameter of Cable/mm	Stress Level	Slip Occurrence		Failure	
					Time/min	Temperature/°C	Time/min	Temperature/°C
H-0.3	Zn-Cu alloy	ø5.15–127	67	0.3	65	346	71	387
H-0.4		ø5.15–127	67	0.4	57	334	61	374

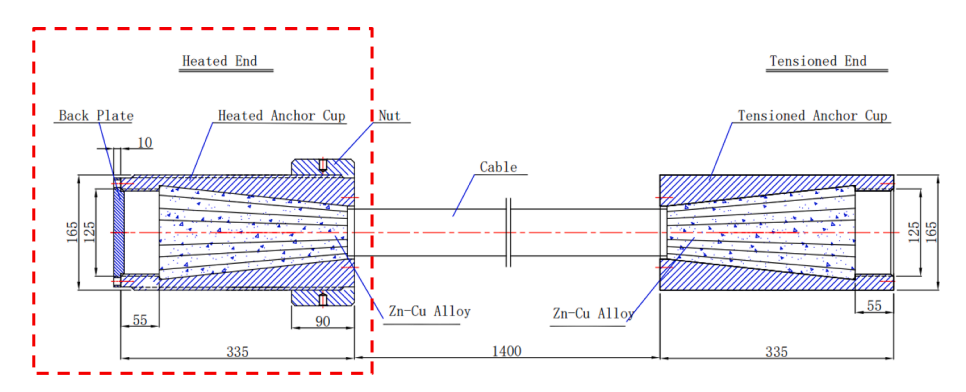


Fig. 1. Design and Dimension of Specimens. (Unit: mm).

noted that the conclusion of Ridge is based on the high-temperature load environment for a long time, which is different from the usual fire environment. And the research results have been adopted by the British specification *BS EN 13411–4: 2011* [18].

Based on the heat conduction theory and ABAQUS software, Du (2019) et al. [15] simulated the transient temperature field distribution of cable sockets under iSO-834 standard fire, and the formulas for calculating the specific heat capacity and thermal conductivity of hotcast anchor filler Zn-Cu alloy and cold-cast anchor filler epoxy resinsteel shot mixture were proposed. Liu (2021) et al. [16] researched the bonding properties and failure mechanism between Galfan-coated steel wire and hot casting material at room temperature and high temperature. The stress transfer of the Galfan-coated steel wire-hot-cast material interface during the steel wire-drawing process was investigated, and a partial-debonding model was given. Hou (2014) et al. [17] researched the degradation law of anchorage performance of prestressed steel bar clamp anchors under fire. The results show that the anchorage system is destroyed when the temperature is higher than 400 °C, and the holding capacity of the anchorage is lost after the temperature is higher than 200 °C.

In summary, research on the high-temperature properties and failure process of hot-cast anchor sockets have not been conducted extensively. And the fire resistance design of the cable anchor sockets has been

imperative. Therefore, this paper conducts in-depth research on the transient temperature field distribution and the degradation law of anchorage performance of the Zn-Cu alloy filled hot-cast anchor sockets. First, two full-scale specimens were heated and loaded to test the transient temperature field distribution and the critical temperature of the hot-cast anchor sockets. Then, the effects of specimen dimensions, steel wire bundle specifications, and heating curves on fire resistance are assessed through numerical modeling using ABAQUS. The fire endurance of hot-cast anchor sockets under different conditions is analyzed to provide a valid basis for fire resistance designing of hot-cast anchor sockets.

#### 2. Experiment

## 2.1. Specimens design

Two full-dimension hot-cast socket specimens with cylindrical appearance and conical cavity are used for the experiments. The specimen details are shown in Table 1. The filling material is Zn-Cu alloy (containing 2 % Cu), the specification of the cable is  $\emptyset$ 5.15–127, and the nominal diameter is 67 mm. The cable is high-strength galvanized parallel wire bundle, and the tensile strength is 1670 MPa. Two stress levels (0.3 and 0.4) are included in the test which is defined as the ratio



(a) Anchor socket before filling



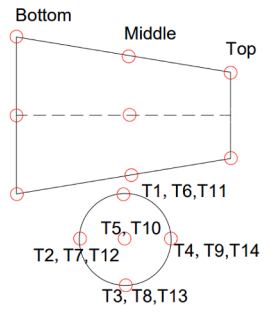
(b) Pouring Zn-Cu alloy



(c) Anchor socket after filling

Fig. 2. Construction Process of Filling Media.







(a) Thermocouple tied to steel wires

- (b) Thermocouple position
- (c) Leading out the thermocouple wires

Fig. 3. Layout of Thermocouples.

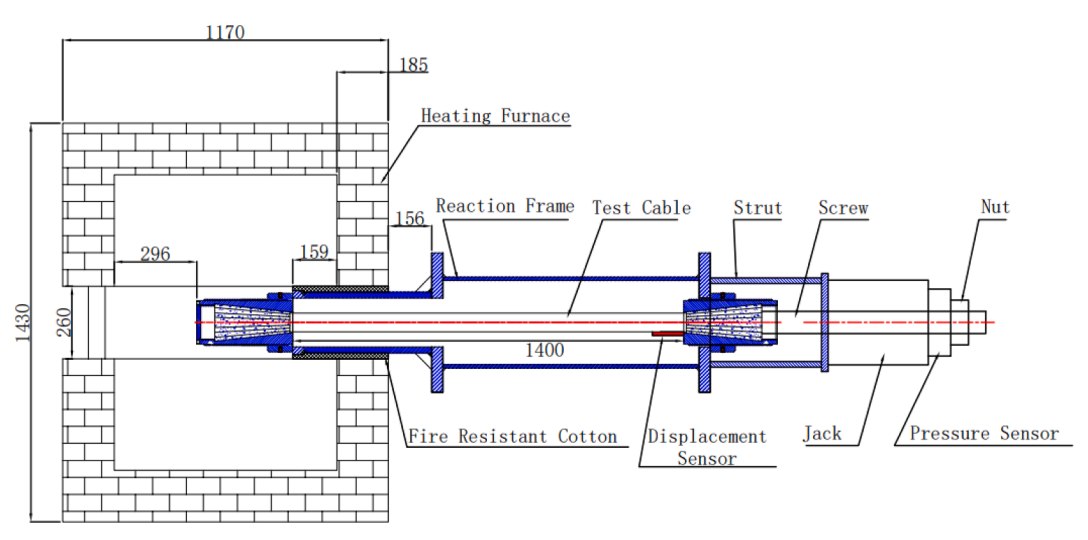


Fig. 4. Schematic Diagram of the Test Device.

of applied tensile load to the ultimate tensile load of the cable, namely the product of the tensile strength and the area of the cable. The prestressed cable has an anchor socket at the tension end and the heating end, separately. The design and dimensions of the specimens are shown in Fig. 1.

# 2.2. Fabrication of specimens and layout of thermocouples

The specimens were produced at Shanghai Pujiang Cable Co., Ltd. Before the end part of the wire bundle was set in the anchor socket, the steel wires were treated to remove grease and sundries. After that melted Zn-Cu alloy solution with a temperature of 460  $^{\circ}$ C was poured into the anchor socket. After it was naturally cooled, the steel wires were bonded to the Zn-Cu alloy. The construction process of the Zn-Cu alloy filler in the anchor socket is shown in Fig. 2.

Before casting, the thermocouples were tied on the steel wire to measure the temperature distribution in the anchorage system (Fig. 3 (a)). A total of 14 thermocouples (T1-T14) were installed on the steel wire bundle, monitoring the temperature change along the axial and radial directions (Fig. 3(b)). The thermocouple wires were led out by punching holes in the cover plate, as shown in Fig. 3(c).

# 2.3. Test device and loading scheme

The experimental equipment consists of the heating furnace, loading frame, jack, oil pressure system, power supply system, control system, and data acquisition system. The full view of the test setup is shown in Fig. 4. The dimension of the electric heating furnace is  $800 \text{ mm} \times 800$ 

 $mm \times 400$  mm, and the rated power is 90 kW. The temperature of the furnace is measured by two S-scale thermocouples arranged in the furnace, and the rising temperature is controlled by intelligent PID (Proportional Integral Derivative). The following test procedure was adopted:

- (1). Install the cable. The specimen was installed according to the position shown in Fig. 4. The heating end of the cable was placed in the electric furnace and the tension end was connected with the jack. Some protective materials were piled at the bottom of the electric heating furnace to protect the equipment.
- (2). Connect the instruments. Connect the thermocouples, pressure sensors, and displacement sensors to the data acquisition system and debug it. Displacement sensor was installed at the front of the tension end to measure the slipping displacement of the heating end at elevated temperature. As shown in Fig. 4, when the stress level keeps constant, the displacement between the tension end and the heating end will only come from the slippage of the heating end due to the elevated temperature.
- (3). Apply tension force. The jack was used to stretch the cable to the predetermined stress level with a speed of 50kN/min and hold the force for 30 min to provide a stable prestress and a reliable zero point of deformation measurement.
- (4). Heating of the specimens. The large space fire formula provided by CECS 200 [19] was used to simulate the fire, in which  $T_z = 680^{\circ}\text{C}$ ,  $\eta = 0.8$ ,  $\mu = 1.0$ ,  $\beta = 0.0018$ . During the heating process, the stress level was kept stable by adjusting the oil pressure.





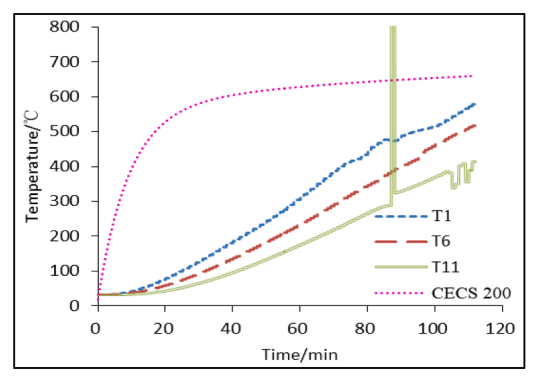


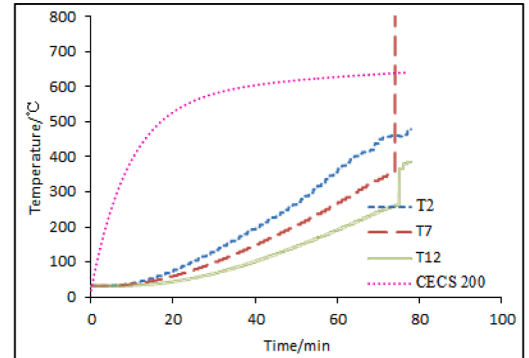
(a) Melted Zn-Cu alloy

(b) Inside of the socket after cooling

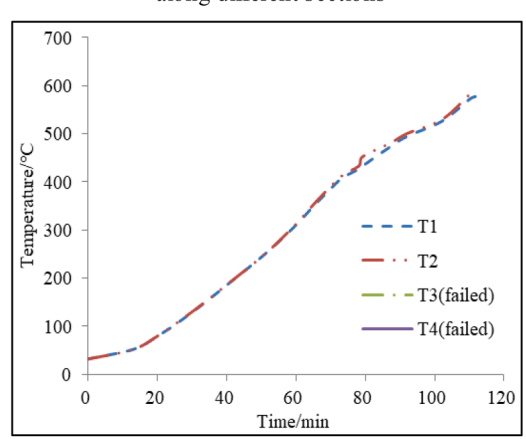
(c) Slip of the cable

Fig. 5. Failure of Hot-Cast Anchor Socket Specimens.

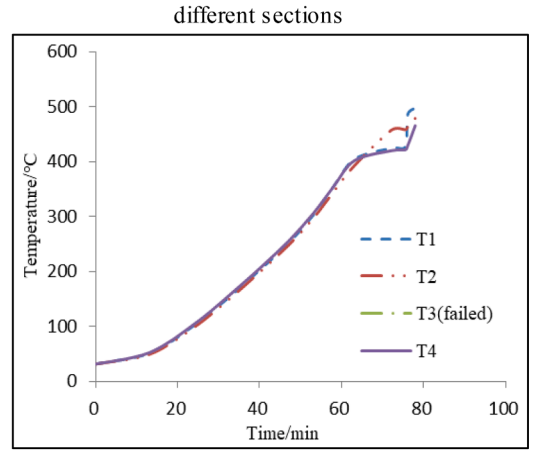




(a) Specimen H-0.3 temperature distribution along different sections



(b) Specimen H-0.4 temperature distribution along



(c) Specimen H-0.3 temperature distribution of bottom sections

(d) Specimen H-0.4 temperature distribution of bottom sections

Fig. 6. Temperature-Time Curves in Specimens.

(5). End the experiment. When the slip of the cable increased rapidly and showed no-convergence, tests were terminated.

# 3. Test results and analysis

# 3.1. Test phenomenon and failure mode

At the initial stage of heating, the specimens changed slightly. When the specimens H-0.3 and H-0.4 were heated for 80 min and 70 min respectively, melted Zn-Cu alloy was observed to flow out of the anchor

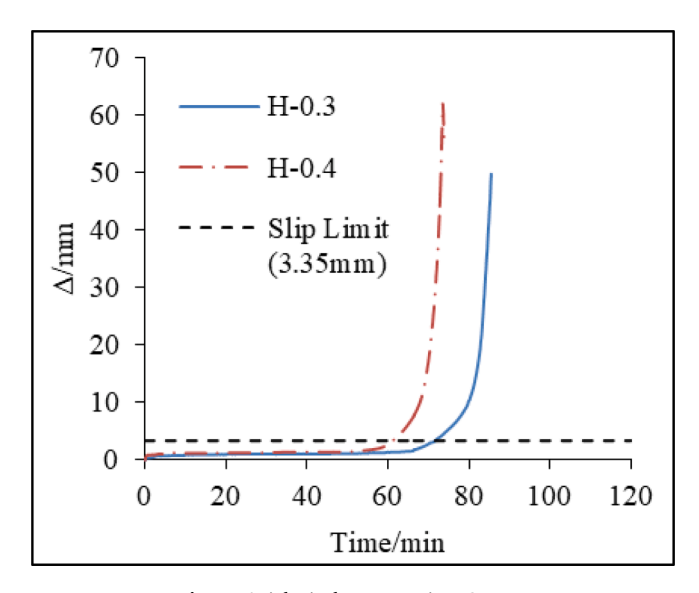


Fig. 7. Axial Displacement-Time Curves.

sockets (see Fig. 5(a)). And then the cable slip increased sharply and the tests were terminated immediately. After cooling, it was found that the Zn-Cu alloy at the bottom of the anchor sockets has melted (see Fig. 5 (b)), but the alloy at the top is still bonded with the steel wire and had been moved out of the anchor sockets under the action of tension (see Fig. 5(c)).

#### 3.2. Temperature-time curves

The internal temperature of the specimens was measured by the thermocouples tied to the steel wires. It should be mentioned that some of the thermocouples failed in the test. In general, the temperature data obtained from the thermocouples can reflect the variation rules of the temperature in the specimens. Fig. 6 shows the temperature-time curves of different measure points. As shown in Fig. 6(a and b), the temperature at the bottom of the anchor socket is higher than that at the middle and top. This is because the outer wall at the bottom of the anchor socket is the thinnest, and heat can be transferred inward through the anchor basket wall and the rear cover plate at the same time. Therefore, the temperature of Zn-Cu alloy at the bottom of the socket is regarded as the critical temperature of the specimens when slip failure occurs.

Five temperature measuring points were arranged at the bottom section of the anchor basket. Due to the failure of some thermocouples, only parts of the curves are shown in Fig. 6(c and d). From Fig. 6(c and d), it can be seen that temperature-time curves are almost identical, indicating that the temperature fields of the alloy are uniformly distributed along the circumferential direction. In (Fig. 6(d)), most of the temperature curves are continuous and smooth, and the curves begin to fluctuate or jump when the temperature is close to the melting point of the Zn-Cu alloy. Due to the existence of tension in the whole process, these points of temperature discontinuity correspond to points where there is a sharp increase in cable slip indicating that the specimens have entered a failure condition.

#### 3.3. Slip displacement-time curves

The slip displacement-time relationship curves of the hot-cast anchor socket specimens are shown in Fig. 7. As can be seen from the figure, the whole slip process can be divided into 3 stages: the no-slip stage, the stable slip growth stage and the sharp slip acceleration stage.

The Zn-Cu alloy filled hot-cast anchor sockets mainly rely on the bonding force between the alloy and the steel wire to transmit the tensile force. At the initial stage of heating, the properties of Zn-Cu alloy inside

the anchor basket are stable, and no slip of the cable occurs. It can be found in Fig. 7 that the time when the specimens H-0.3 and H-0.4 starts to slip is 65 min and 57 min respectively, and the corresponding temperature of the Zn-Cu alloy at the bottom of the specimen are 346 °C and 334  $^{\circ}$ C respectively. It can be inferred that the bonding force between the alloy and the steel wire starts to degrade at about 340 °C and the sliptime curves enter the second stage. The second stage is the slip generation and development stage. When the temperature of the Zn-Cu alloy at the bottom of the anchor basket exceeds 340 °C, the temperature of the alloy in the rest of the anchor basket is still below 340 °C. Therefore, most of the bonding force between the steel wire and the alloy is still maintained, which makes the slip of the hot-cast anchor sockets develop steadily, and the duration of this stage is about 10 min. The third stage is the destructive stage. When the temperature of the alloy at the bottom end exceeds 420 °C and starts to melt, the bonding force between the alloy and the steel wires is almost lost, the slip grows sharply and the anchorage system is completely destroyed.

The anchorage system is considered to be damaged when the slip reaches 1/2 of the nominal diameter of the cable by Ridge (2012) et al. [5]. In this research, the slip limit of the Zn-Cu alloy anchor sockets is conservatively taken as 5 % of the nominal diameter of the cable ( i.e. 3.35 mm in this test as shown in the dashed line in Fig. 7). According to this damage criterion, the failure time of specimen H-0.3 is 71 min, and the corresponding temperature at the inner wall of the socket bottom is 387  $^{\circ}$ C. For specimen H-0.4, the final damage duration is 61 min, and the temperature at the inner wall of the socket bottom is 374  $^{\circ}$ C. So the critical temperature of the specimens in this test when damage occurs is 374 °C – 387 °C. It was found that the stress level had an influence on fire resistance of the specimens. When the stress level increased from 0.3 to 0.4, the fire endurance of the specimens reduced from 71 min to 61 min and the critical temperature decreased from 387°C to 374 °C. Due to the limited number of specimens in this test, the correlation between critical temperature and stress level cannot be given accurately. It is suggested that the critical temperature can be conservatively taken as 350 °C for the hot cast anchor specimens.

## 4. Numerical analysis of temperature field

#### 4.1. Thermophysical parameters of hot-cast anchor sockets

The hot-cast anchor filler is Zn-Cu alloy, which is composed of 98 % Zn and 2 % Cu. The density  $\rho_r = 6930 \text{kg/m}^3$ , the thermal conductivity  $\lambda_r$  and specific heat capacity  $C_r$  of Zn-Cu alloy vary in many stages with temperature, the fitting results of  $\lambda_r$  in W/(m·°C) and  $C_r$  in J/(kg·°C) in reference [15] are as formulas (1) and (2):

$$\lambda_{r} = \begin{cases} 99.47 - 0.016\theta + \frac{79.48}{\theta^{2}}, 25^{\circ} C \leq \theta < 200^{\circ} C \\ 96.3, 200^{\circ} C \leq \theta \leq 250^{\circ} C \\ 52.92 + 1.92\theta^{0.5} + 3287.93/\theta, 250^{\circ} C < \theta \leq 400^{\circ} C \end{cases}$$
(1)

$$C_{r} = \begin{cases} 428.21 - 0.0003\theta^{1.5} - 1582.24/\theta + 18818.68/\theta^{2}, 25^{\circ} C \leq \theta < 150^{\circ} C \\ 177.97 + 9.66\theta^{0.5} + 1490.56/\theta^{0.5}, 150^{\circ} C \leq \theta \leq 250^{\circ} C \\ 653.12 - 0.00014\theta^{2} - 99450/\theta + \frac{11146153.85}{\theta^{2}}, 250^{\circ} C < \theta \leq 400^{\circ} C \end{cases}$$

$$(2)$$

Above formulas:  $\theta$ , is the temperature of Zn-Cu alloy (°C).

The material of the anchor socket is steel and the thermophysical property is taken according to EN 1993-1-2 [20]. The density of steel  $\rho_a = 7850 \text{kg/m}^3$ , the specific heat capacity  $C_a$  in J/(kg·°C) and thermal conductivity  $\lambda_a$  in W/(m·°C) of steel is obtained from the formulas (3) and (4):

$$C_a = 425 + 7.73 \times 10^{-1} \theta_a - 1.69 \times 10^{-3} \theta_a^2 + 2.22 \times 10^{-6} \theta_a^3$$
 (3)

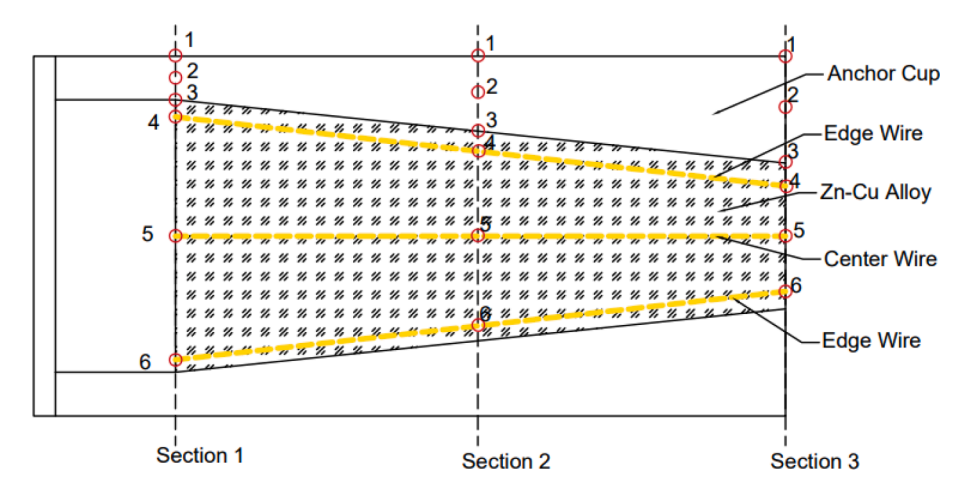


Fig. 8. Model Measurement Point Layout.

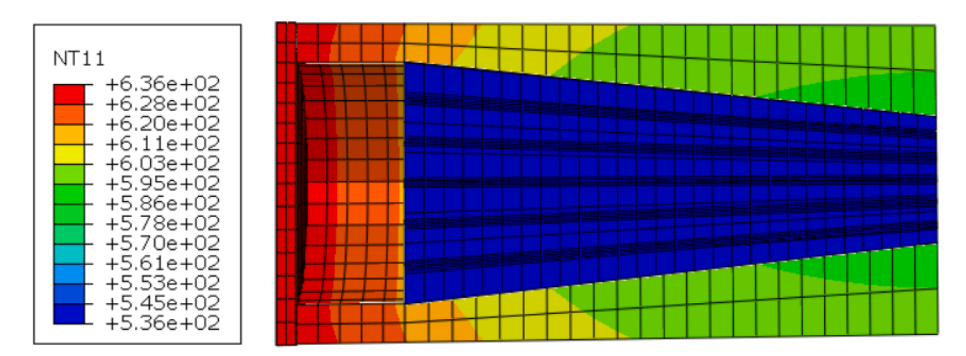


Fig. 9. Temperature Cloud Map of Hot-Cast Anchor.

$$\lambda_a = 54 - 3.33 \times 10^{-2} \theta_a \tag{4}$$

Above formulas: $\theta_a$ , is the temperature of steel (°C).

#### 4.2. Numerical heat transfer simulation

The heat transfer process is composed of three basic modes: heat conduction, convection, and radiation. When the structure suffers from a fire, the hot air transfers heat to the surface of the specimen through convection and radiation, while the interior of the structure mainly transfers heat employing heat conduction.

The model measurement points are arranged as shown in Fig. 8, in which points 1-2 are on the anchor socket wall, point 3 is on the interface between the anchor socket inner wall and the filling, and points 4–6 are corresponding to the test measurement points. The points of different sections are used to measure the longitudinal temperature change of the specimens. Taking the large space heating curve (CECS 200) [19] as the boundary condition, the 8-node linear hexahedral element (DC3D8) in the ABAQUS numerical heat transfer simulation platform is used for Zn-Cu alloy filler, anchor socket wall, and embedded steel wire. The fire condition is the "fire" on the anchor socket wall and the back cover, the surface heat exchange and surface radiation conditions are set on the "fire" surface, and the convective conductivity coefficient is 25 W/( $m^2$ ·K), the radiation coefficient is 0.5, the absolute zero is -273 °C, and the Stefan-Boltzmann constant is  $5.67 \times 10^{-8}$  W/  $(m^2 \cdot K^4)$ . The steel wires were embedded in the Zn-Cu alloy by using the command "Embedded Region". Constraint binding among the components of the hot-cast anchor sockets is set by using the command "Surface-to-Surface Contact", and the value of contact thermal resistance is  $0.012 \, (\text{m}^2 \cdot \text{K/W}).$ 

# 4.3. Numerical simulation results under CECS 200

The temperature cloud map of hot-cast anchor under CECS 200 is shown in Fig. 9. The results of three-dimensional numerical heat transfer analysis for different measuring points for specimen H-0.4 are shown in Fig. 10. Fig. 10(a - c) show the temperature curves for each measurement point in sections 1, 2 and 3, respectively. Therefore, there is a certain hysteresis temperature difference between the anchor and the filler. The temperature of the Zn-Cu alloy is significantly lower than that of the anchor socket due to the thermal resistance contact between the two materials. This study pays more attention to the temperature of the Zn-Cu alloy filler, so the measuring point 4 with higher temperature in the filler is taken as the research object. Fig. 10(d) compares the heating curves of the bottom measurement point 4 from the experiment and the simulation results. When the critical temperature of 350 °C is reached, the time required for the experiment and simulation is 57 min and 65 min respectively. The analysis shows that the simulation results of the temperature field are basically consistent with the test data, and the heat transfer model is reliable, which increases the credibility of the parametric analysis.

#### 4.4. Parametric analysis

Effects of parameters such as the heating curves, specimen dimensions, and steel wire bundle types on the fire performance of the specimens are discussed in this section. Three more heating curves including iSO-834, HC, and ASTM E119 are considered, along with CECS 200, as shown in Fig. 11. Dimensions of two test specimens are regarded as the reference values, then the selected specimen dimensions are enlarged by 1.2, 1.4, and 1.6 times. For example, when the dimensions are magnified 1.2 times, it can be expressed as: the length is  $335 \times 1.2$ 

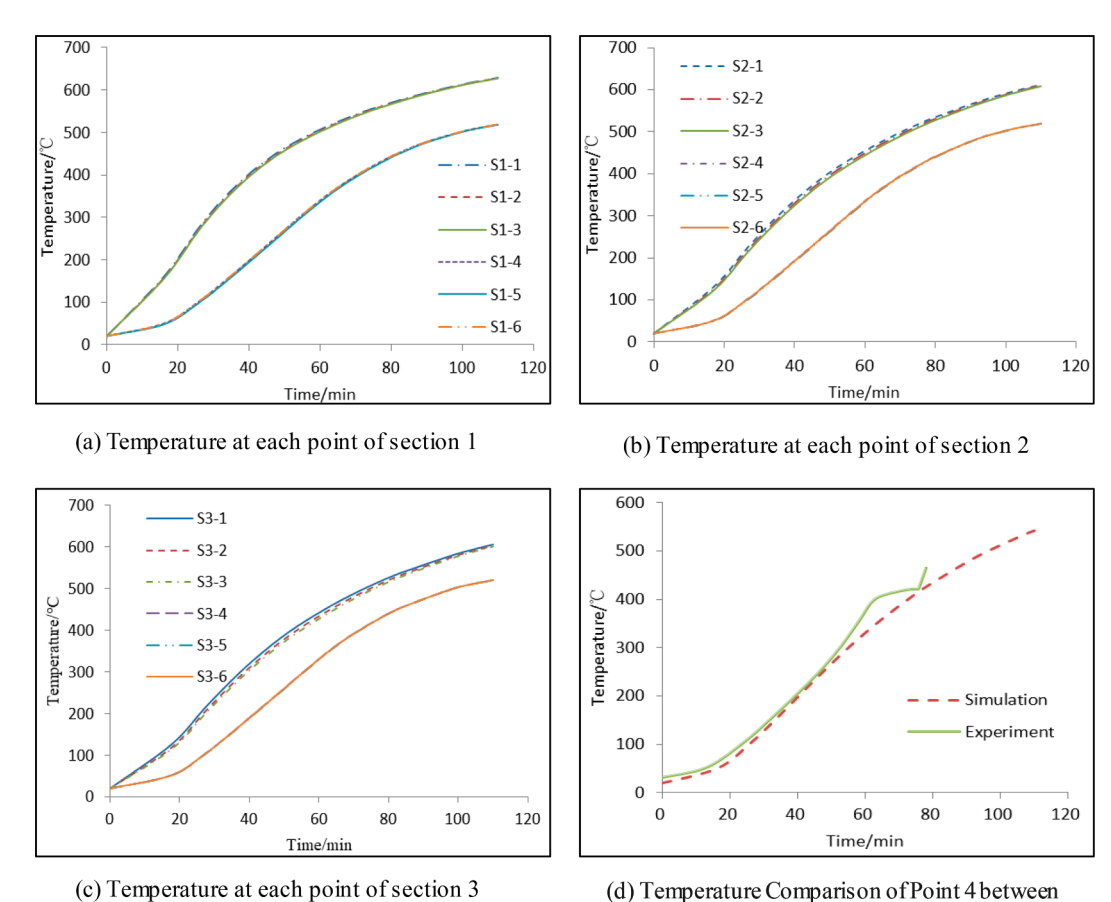


Fig. 10. Temperature Profiles of Measurement Points on Different Sections.

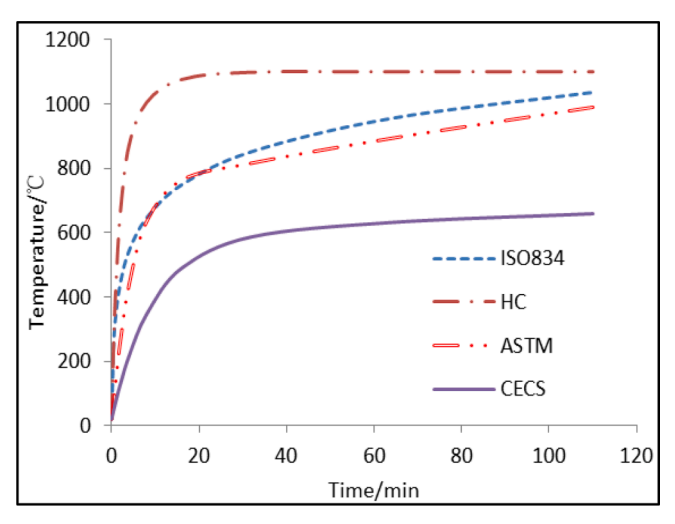


Fig. 11. Four Temperature-Time Curves.

mm, the diameter is  $165\times1.2$  mm, the top thickness of the anchor basket is  $49\times1.2$  mm, and the bottom thickness of the anchor basket is  $20\times1.2$  mm. Besides the steel wire bundle of 5 mm  $\times$  91, those of 6.2 mm  $\times$  61 and 7.7 mm  $\times$  37 commonly used in engineering are selected to consider the effect of the steel wire bundle types, that is, the effect of the diameter and number of the steel wire when the area of the steel wire bundle is similar.

A total of 48 specimens with different parameters are analyzed. The time when their measuring point 4 reaches 350  $^{\circ}\text{C}$  is provided in Table 2.

From the data in the table, it can be concluded that the heating curves and specimen dimensions have significant effects on fire endurance of the specimens, whereas the effect of steel wire bundle types can be neglected. When exposed to HC temperature–time curve, the specimens need 26 min to reach the critical temperature, which is only 40 % of 65 min corresponding to CECS 200 curve. The fire endurance of the specimens are similar when the heating curves followed iSO-834 and ASTM E119.

Experiment and Simulation

In order to more clearly show the influence of the dimenions, the temperature-time curves of specimens with different dimenions are plotted in Fig. 12. Specimen ID in this figure is defined as follows: the letter represents the temperature-time curves, the first group of numbers represents the dimension magnification times, and the second group of numbers represents the diameter of the steel wire. For instance, I-1.2–5 represents the heating curve is followed ISO 834, the dimension becomes 1.2 times of the reference value, and the steel wire diameter is 5 mm. It is obvious that the larger the specimen dimensions, the better fire resistance. For every 10 % increase in specimen dimensions, the average increase rate of fire endurance is about 6 % ~7%. When the specimens are exposed to the HC heating curve, the average increase rate of fire endurance is 7 %, and the value is around 6 % for the other three heating curves. It can be inferred that if the fire resistance of the specimens is improved by increasing the dimensions, the improvement effect for specimens under the HC heating curve will be more obvious than that for specimens under the other three heating curves.

#### 5. Conclusions

Two full-scale specimens were heated and loaded to research the transient temperature field distribution and the degradation law of

Table 2 Time to reach 350  $^{\circ}$ C of measuring Point 4 for 48 specimens.

Temperature Curve	Wire Diameter/mm	n Magnification							
		1	1.2		1.4		1.6		
		Time/min	Time/min	Average Increase rate	Time/min	Average Increase rate	Time/min	Average Increase rate	
ASTM E119	5	39	43.8	12.64 %	48.6	25.11 %	53.5	37.58 %	
	6.2	39.3	43.5		48.3		53		
	7.7	38	43.7		48.6		53.5		
CECS 200	5	65	72	11.92 %	80.2	24.46 %	88	36.94 %	
	6.2	65	72		80		88.2		
	7.7	63	72		80		88.1		
НС	5	23	26.3	14.35 %	29.3	27.54 %	32.7	42.17 %	
	6.2	23.3	26.4		29.5		32.9		
	7.7	22.7	26.2		29.2		32.5		
ISO 834	5	37.5	42	12.7 %	46.5	24.87 %	51	37.21 %	
	6.2	37.6	42		46.6		51.4		
	7.7	36.7	42		46.5		51		

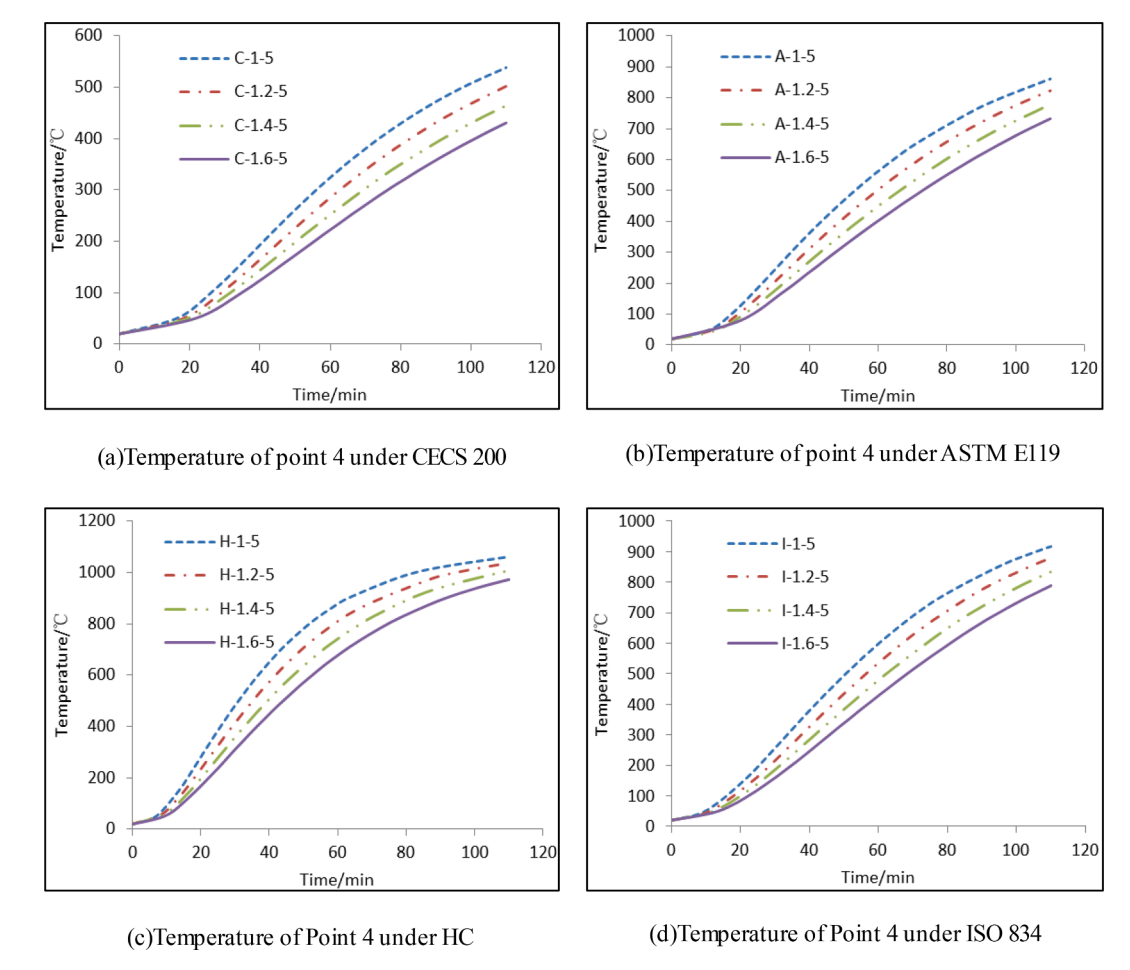


Fig. 12. Effect of Specimen Dimensions on the Temperature of Measuring Point 4.

anchorage performance of the Zn-Cu alloy filled hot-cast anchor sockets. Based on the experimental results, a numerical model was developed in ABAQUS and validated for parametric study, in which the effects of specimen dimensions, steel wire bundle types and the heating curves are assessed. The conclusions of this study are as follows:

- (1) The temperature distribution inside the sockets is uneven and the bottom temperature is the highest. Therefore, the temperature of Zn-Cu alloy at the bottom of the sockets is regarded as the critical temperature when slip failure occurs.
- (2) The slip of cable anchorage system under fire can be divided into three stages: no slip stage, stable and rapid growth stages of the slip. The anchorage system is considered to be damaged when the

- slip reaches 5 % of the nominal diameter of the cable in this paper, which corresponds to the stable growth stage of slip.
- (3) Stress level has influence on fire resistance of the specimens. When the stress level increased from 0.3 to 0.4, the fire endurance of the specimens reduced from 71 min to 61 min and the critical temperature decreased from 387 °C to 374 °C. Howerver, the correlation between critical temperature and stress level cannot be given accurately due to the limited number of specimens. Thus the critical temperature is uniformly taken as 350 °C for the hotcast specimens in this paper.
- (4) Numerical simulation results show that the effect of the diameter and number of the steel wire is slight when the area of the cable is similar, whereas the effect of heating curves and specimen dimensions is significant.
- (5) Specimens with larger dimensions show better fire resistance. For every 10 % increase in specimen dimensions, the average increase rate of fire endurance is about 6 % ~7%. Compared with the other three heating curves, changing the dimensions has the most obvious effect on fire endurance of the specimen exposed to HC heating curve.

#### **Declaration of Competing Interest**

The authors declare that they have no known competing financial interests or personal relationships that could have appeared to influence the work reported in this paper.

#### Acknowledgements

This work was financially supported by Shanghai Natural Science Foundation (18ZR1427900,22ZR1446400). The financial support is appreciated.

#### References

 Atienza JM, Elices M. Behavior of prestressing steels after a simulated fire: Fireinduced damages. Constr Build Mater 2009;23(8):2932–40.

- [2] Yoo H, Lee SH, Lee JK. Mechanism of bonding between Zn–Al-coated wires and Zn–Cu alloy casting medium in hot casting socket terminations for large bridge cables. Constr Build Mater 2015;76:396–403.
- [3] Wang L-C, Zhang J-Y, Xu J, Han Q-H. Anchorage systems of CFRP cables in cable structures-a review. Constr Build Mater 2017;160:82–99.
- [4] Klein TW. The security assessment of cable assemblies in structures. The International Bridge Conference (IBC 2008), 2nd-4th June, Pittsburgh, PA USA, paper IBC 08-30.
- [5] Ridge I, Hobbs R. The behaviour of cast rope sockets at elevated temperatures. J Struct Fire Eng 2012;3:155–68.
- [6] Bennetts I, Moinuddin K. Evaluation of the impact of potential fire scenarios on structural elements of a cable-stayed bridge. J Fire Prot Eng 2009;19(2):85–106.
- [7] Du Y, Li G-Q. A new temperature-time curve for fire-resistance analysis of structures. Fire Safety J 2012;54:113–20.
- [8] Zhang G-W, Zhu G-Q, Yin F. A whole process prediction method for temperature field of fire smoke in large spaces. Pro Eng 2014;71:310-5.
- [9] Kotsovinos P, Atalioti A, McSwiney N, Lugaresi F, Rein G, Sadowski AJ. Analysis of the thermomechanical response of structural cables subject to fire. Fire Tech 2020; 56(2):515–43.
- [10] Chen W, Shen R. Study of temperature field inhomogeneities in parallel wire strand sections under ISO834 fire. Ksce J Civ Eng 2021;25(10):3940–52.
- [11] Fontanari V, Benedetti M, Monelli BD, Degasperi F. Fire behavior of steel wire ropes: Experimental investigation and numerical analysis. Eng Struct 2015;84: 340-9.
- [12] Du Y, Peng J-Z, Richard Liew JY, Li G-Q. Mechanical properties of high tensile steel cables at elevated temperatures. Constr Build Mater 2015;182:52–65.
- [13] Shakya AM, Kodur VKR. Effect of temperature on the mechanical properties of low relaxation seven-wire prestressing strand. Constr Build Mater 2016;124:74–84.
- [14] Agrawal AK, Gong X. Safety of cable-supported bridges during fire hazards. J Bridge Eng 2016;21:04015082.
- [15] Du Y, Zhu Y, Jiang J, Li G-Q. Transient temperature distribution in pre-tensioned anchors of cable-supported structures under ISO834 fire. Thin Wall Struct 2019; 138:231–42.
- [16] Liu H-B, Guo L-L, Chen Z-H, Meng Y-D, Zhang Y-J. Study on bonding mechanism of hot-cast anchorage of galfan-coated steel cables. Eng Struct 2021;246:112980.
- [17] Hou X-M, Zheng W, Sun H. Research on deterioration of anchoring performance between anchorages to steel bars for prestressed concrete under fire. J Build Struct 2014;35:110–8. in Chinese.
- [18] BS EN 13411-4-2011. Terminations for steel wire ropes-safety-safety-Part 4: Metal and resin socketing. British Standards Institution 2011.
- [19] CECS 200-2006. Technical code for fire safety of steel structure in buildings. China Association for Engineering Construction Standardization 2006.(in Chinese).
- [20] EN 1993-1-2, Eurocode 3: Design of steel structures Part 1-2: General rules Structural fire design. European Committee for Standardization 2005.